Okulov, A.V.; Volegov, A.S.; Weissmueller, J.; Markmann, J.; Okulov, I.V.:
Dealloying-based metal-polymer composites for biomedical applications
In: Scripta Materialia 146 (2018) 290 - 294
First published online by Elsevier: December 21, 2017

DOI: 10.1016/j.scriptamat.2017.12.022
https://dx.doi.org/10.1016/j.scriptamat.2017.12.022

Dealloying-based metal-polymer composites for biomedical applications

A.V. Okulov[a], A. S. Volegov[b], J. Weissmüller[a,c], J. Markmann[a,c], I.V. Okulov[a]*

[a] *Helmholtz-Zentrum Geesthacht, Institute of Materials Research, Division of Materials Mechanics, 21502 Geesthacht, Germany*

[b] *Ural Federal University, Institute of Natural Sciences and Mathematics, 620002 Yekaterinburg, Russia*

[c] *Institute of Materials Physics and Technology, Hamburg University of Technology, 21073 Hamburg, Germany*

**Corresponding author. E-mail: ilya.okulov@hzg.de.*

Abstract

Here, we developed interpenetrating-phase metal-polymer composites mimicking mechanical behavior of cortical bone and occupying previously unclaimed region at the Ashby diagram in the area of intermediate strength and low stiffness. The composites consist of dealloying-based open porous Ti_xHf_{100-x} alloys (scaffolds) impregnated by polymer. The scaffolds significantly contribute to strength (215–266 MPa) and stiffness (15.6–20.8 GPa) of the composites while the polymer phase provides their high strain rate sensitivity (0.037–0.044). Tuning connectivity of scaffolds by preloading allows fine optimization of composites' mechanical properties. The results suggest that the composites may provide a basis for promising future implant materials.

Keywords: Dealloying; Porous material; Composites; Biomaterial; Mechanical properties

Commercially pure titanium and titanium alloys are widely used metallic materials for bone trauma healing, because of their good mechanical performance, excellent biocompatibility, and high corrosion resistance [1–3]. Despite the success of existing commercial implant materials in many cases, there is a risk of bone degeneration and implant loosening caused by the so-called “stress-shielding” effect [2,3]. The “stress-shielding” effect is associated with the disproportional load distribution between a bone and an adjacent implant due to their stiffness mismatch. The metallic implant materials are usually considerably stiffer as compared to bones. Eventually, the stiffness mismatch may lead to bone resorption and the loosening or failure of the implant. Effective strategies to develop low stiffness titanium alloys with reasonably low stiffness include designing of multicomponent titanium alloys with dominating bcc phase [4–6], development of complex nano- and microstructures [7–10] or fabrication of porous structures [11–13]. The infiltration of open porous scaffolds by polymers can lead to a unique combination of mechanical properties attractive for biomedical applications as it was recently reported in [13]. In this case, the biocompatible open porous scaffolds were obtained by the liquid metal dealloying.

The liquid metal dealloying as proposed by Kato and co-workers [14] is a metallurgical process for synthesis of open porous materials by means of selective corrosion in a liquid metal. It employs diffusion of a liquid metal into a precursor material accompanied by selective dissolution of one or several components. The remaining part of the precursor material is immiscible with the liquid metal and rearranges into a continuous scaffold consisting of interconnected ligaments. The size of ligaments of the dealloying-based materials can be effectively tuned from the nano- to the micrometer range by control of the processing conditions [13,15–17]. Currently, a wide range of open porous metallic materials, including Ti [13,14], Fe [18], Zr [13], Cr [18], Nb [16], Ta [19], TiNb [13], and TiZr [13], was developed using the liquid metal dealloying method. Moreover, the method was reported to be effective in surface modification for bio-applications, e.g. patterning of tailorable nanotopographies [20] and selective removal of toxic elements [21]. The interpenetrating-phase materials by liquid metal dealloying offer novel opportunities for load-bearing applications [22] as well as fabrication of advanced implant materials [13].

Here, we report on the synthesis and structure-property correlation of titanium-hafnium (Ti_xHf_{100-x}) open porous alloys and interpenetrating-phase composites obtained by impregnation of the Ti_xHf_{100-x} scaffolds by bisphenol F epoxy resin. The Ti-Hf alloys were selected for this study because of good biocompatibility and osteoconductivity of both Ti and Hf [23]. Moreover, addition of Hf to Ti gradually increases strength of Ti-Hf alloys due to solid solution strengthening [24]. Synthesized by dealloying in liquid magnesium, the open porous Ti_xHf_{100-x} alloys inherit a unique open porous microstructure through manufacturing leading to its outstanding mechanical properties. The mechanical properties of Ti_xHf_{100-x} scaffolds can be flexibly tuned by a preloading treatment providing, for example, the opportunity of precise stiffness adjustment between implant and bone. The impregnation of the open porous Ti_xHf_{100-x} scaffolds by polymer leads to significant strength improvement. The yield strength of the metal-polymer composites exceeds that of cortical bone while its stiffness remains in a range of that for cortical bone. Moreover, the composites exhibit high strain rate sensitivity similar to bone.[1] These findings suggest advantages of the dealloying-based composites for biomedical applications as bioimplants with adjustable mechanical properties.

The design of precursor alloys for the liquid metal dealloying was based on the enthalpy of mixture between Mg and the considered alloying element ($\Delta H^{mix}_{(Mg-element)}$) as well as on biocompatibility of the alloying elements. Elements exhibiting a negative value of $\Delta H^{mix}_{(Mg-element)}$ like Cu are miscible and will be dissolved in Mg upon the dealloying process while those possessing a positive $\Delta H^{mix}_{(Mg-element)}$ like Ti and Hf are immiscible in Mg. Thus, Ti, Hf and Cu were selected for the alloy design because these elements are miscible with each other [25]. Three alloys, namely, $Ti_{20}Hf_{20}Cu_{60}$, $Ti_{25}Hf_{15}Cu_{60}$, and $Ti_{30}Hf_{10}Cu_{60}$ (at.%) were designed in order to identify the effect of Hf on the microstructure as well as the mechanical response of the porous Ti_xHf_{100-x} alloys.

The samples (rods of 1 mm in diameter) for liquid metal dealloying were prepared from pure metals (99.99 %) by a suction casting set-up under argon atmosphere. The rods were

[1] The strain rate values of bone were derived from the stress-strain curves tested at different strain rates by Crowninshiled and Pope [32]

cut to 1.7 mm length by a diamond wire saw and dealloyed at 1023 K for 600 s in Mg in a glassy carbon crucible under argon flow using an infrared furnace (IRF 10, Behr, Switzerland). Upon dealloying, molten Mg selectively dissolves Cu out of the parent $(Ti_xHf_{100-x})_yCu_{100-y}$ alloys, while Ti and Hf diffuse along the metal/liquid interface [14,19]. In order to obtain porous samples, a Mg phase were removed by etching in 3 M HNO_3 for 5 h. The composites were prepared by subjecting the porous metal samples to vacuum for 10 min and then bringing them in contact with the liquid Bisphenol F epoxy resin (BER 20, Buehler, Germany, number average molecular weight ≤ 700 g mol^{-1}) mixed 4:1 with amine hardener (BEH 20, Buehler), using a vacuum impregnation unit (CitoVac, Struers, Germany). The detailed experimental procedure is described in [13].

Fig. 1 illustrates the microstructure of the interpenetrating-phase composites of the bisphenol F epoxy resin (further referred as BPF) and open porous Ti_xHf_{100-x} alloys (Ti_xHf_{100-x}_BPF composites). The polymer phase is hardly visible on the polished surface of the composites what is in agreement with [26]. The blur contrast of the metallic ligaments under the polymer layer directly indicates the presence of the polymer phase. The microstructures of the Ti_xHf_{100-x} scaffolds agree with the uniformly interconnected network structure (Fig. 1). The X-ray diffraction analysis indicated that the porous Ti_xHf_{100-x} alloys are single phase materials and consist of hexagonal close-packed phase (Fig. 2). This is in agreement with the literature, see e.g. the Ti-Hf phase diagram [24,25,27].

The characteristic microstructural parameters of the porous Ti_xHf_{100-x} alloys such as mean ligament sizes, *L*, and volume fraction of metal phase, φ, are listed in Table 1. As it can be seen from the Table 1, the metal volume fraction increases from 54 ± 3 to 59 ± 2 vol.% for $Ti_{75}Hf_{25}$ and $Ti_{50}Hf_{50}$ scaffolds, respectively. Samples exhibit a notable shrinkage during dealloying in a range from 3.9 to 9.8 vol.% (Table 1). The shrinkage is lower for the alloys with higher Hf content. Comparing the shrinkage behavior of the current $(Ti_xHf_{100-x})_{40}Cu_{60}$ alloys and the $Ti_{40}Cu_{60}$ alloy in Mg [13], it can be concluded that Hf additions can be used for suppressing shrinkage during dealloying. The shrinkage influences solid fraction and, therefore, the mass-density of the porous scaffolds. The current porous Ti_xHf_{100-x} alloys possess low mass density values in a range from 3.9 to 5.1 g cm^{-3} (Table 1).

The porous Ti_xHf_{100-x} alloys can be classified as an ultrafine-structured material according to its fine microstructural features. The mean ligament size varies from 0.67 ± 0.11 μm to 0.79 ± 0.12 μm slightly increasing with higher Hf content. These values are notably lower compared to those reported for dealloying-based porous Ti [13]. This suggests that Hf additions are useful for the microstructural refinement of dealloying-based porous titanium. The smallest interligament spacing of about 230 ± 90 nm corresponds to the porous $Ti_{75}Hf_{25}$ with the smallest ligament size (Table 1). Larger magnification of the microstructure resolves some more notable features. The ligaments consist of rounded particles joint to each other similar to a sintering microstructure (Figs. 1 a and b).

As detailed above, open porous Ti_xHf_{100-x} samples were vacuum-impregnated with the bisphenol F epoxy resin (BPF). As a small chain-length resin, BPF has low viscosity, facilitating impregnation. It has already been shown for nanoporous gold and was confirmed by the fact that we could effectively polish the samples without destroying its internal structure, the vacuum impregnation achieves complete filling of the entire pore space with no voids [28]. This also was confirmed here by the analysis of the loading-unloading mechanical tests, discussed below.

Table 1. Microstructural characteristics of the porous Ti_xHf_{100-x} alloys

Composition (at%)	**Solid fraction [vol.%]**	**Ligament size [μm]**	**Interligament spacing [μm]**	**Shrinkage [vol%]**	**Density [g cm^{-3}]**
$Ti_{50}Hf_{50}$	59±2	0.79±0.12	0.33±0.14	3.9	5.1±0.2
$Ti_{62.5}Hf_{37.5}$	54±3	0.71± 0.18	0.36±0.14	4.8	4.4±0.2
$Ti_{75}Hf_{25}$	55±3	0.67±0.11	0.23±0.09	9.6	3.9±0.1

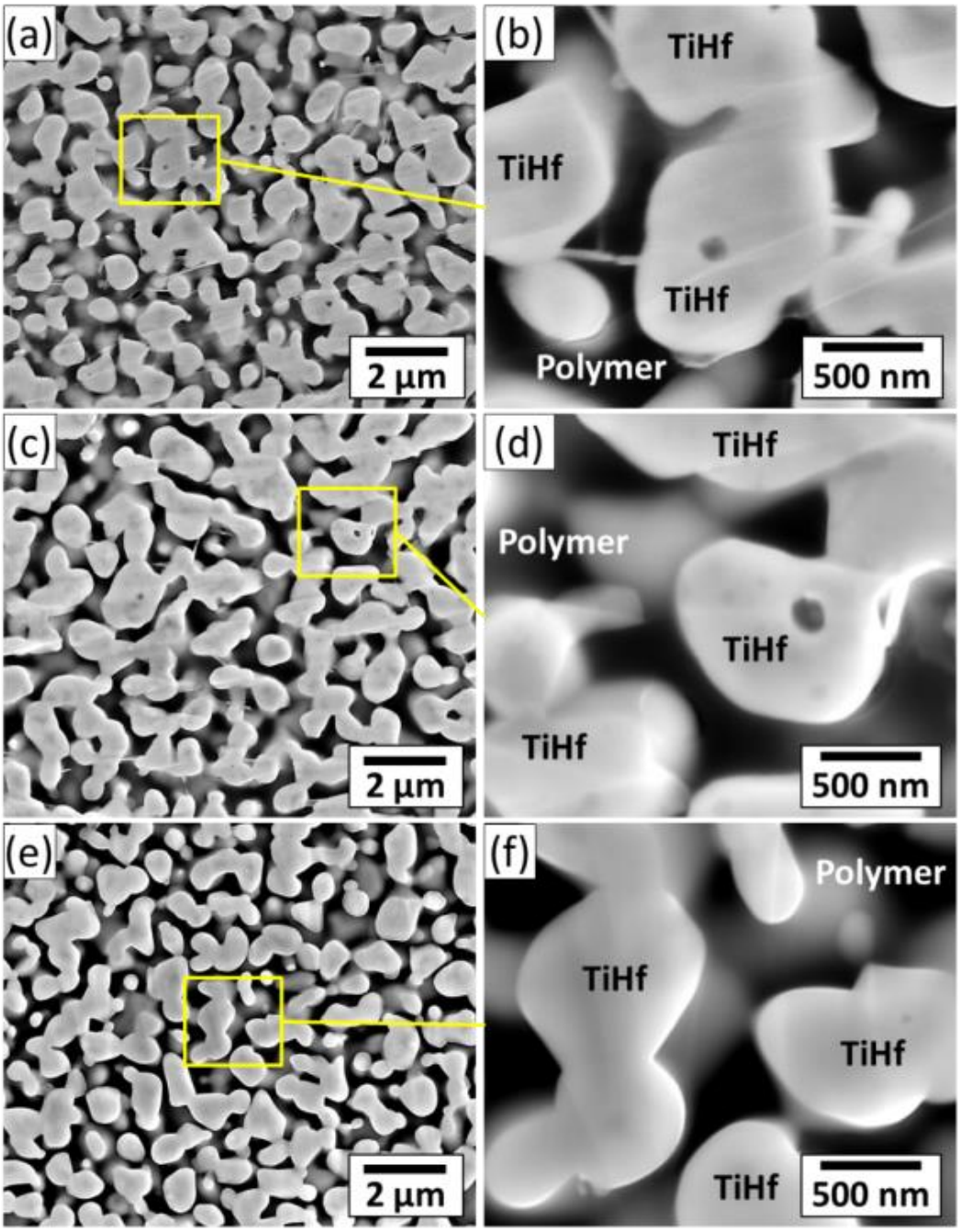

Fig. 1 Microstructure of the interpenetrating-phase Ti_xHf_{100-x}_BPF composites. (a, b) $Ti_{50}Hf_{50}$_BPF; (c, d) $Ti_{62.5}Hf_{37.5}$_BPF; and (e, f) $Ti_{75}Hf_{25}$_BPF.

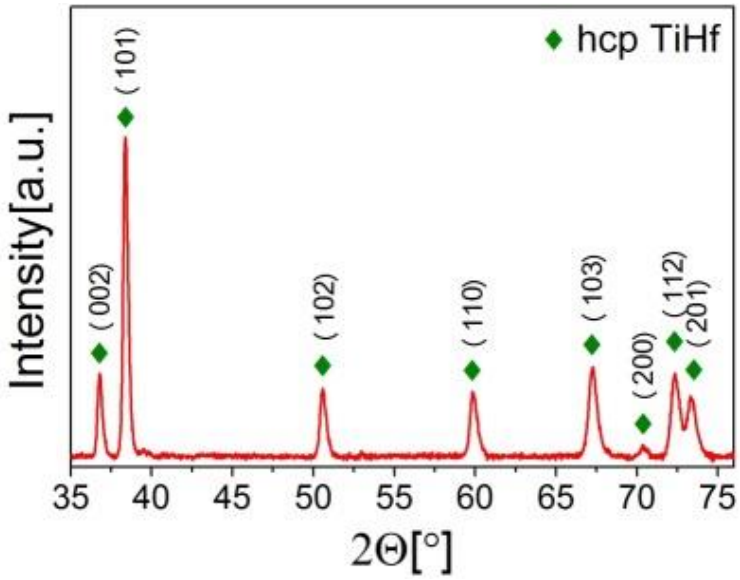

Fig. 2 X-Ray diffractogram of the open porous $Ti_{50}Hf_{50}$ alloy. This is representative for the Ti_xHf_{100-x} alloys synthesized in this study.

The quasi-static mechanical tests of the porous and the composite materials are shown in Fig. 3 a. The porous Ti_xHf_{100-x} alloys exhibit significant plastic deformability with strains of several 10% prior to failure under compressive loading. Consistent with the large plastic deformability of the porous alloys is the pronounced strain-hardening, which promotes uniform plastic flow. The large compressive strains were also reported for a number of open porous metallic materials from nanoporous gold fabricated by electrochemical dealloying [29] to open porous Ti and its alloys fabricated by liquid metal dealloying [13]. The impregnation of the porous scaffolds by polymer leads to decreasing of their fracture strain values. Nonetheless, the interpenetrating-phase metal-polymer composites possess good plastic deformability with strains of about 10% prior to failure. Moreover, the polymer impregnation leads to superior strength characteristics of the composites. The yield strength data of both materials types are summarized in Table 2.

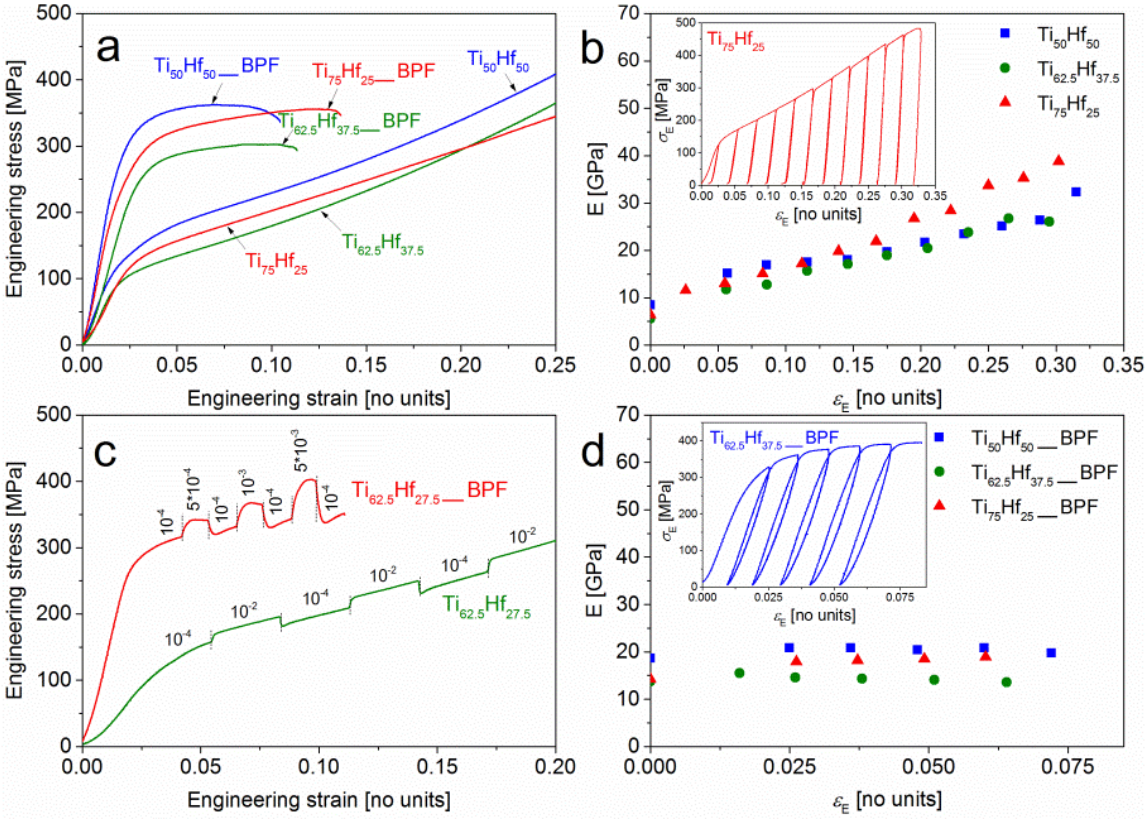

Fig. 3 Mechanical behavior of the open porous Ti_xHf_{100-x} alloys and the interpenetrating-phase Ti_xHf_{100-x}_BPF composites at room temperature, probed under compressive loading. (a) Compressive stress-strain curves; (b) Elastic modulus plotted against engineering strain for the open porous Ti_xHf_{100-x} alloys (Inset: loading-unloading stress-strain curve for $Ti_{75}Hf_{25}$); (c) Strain-rate jump tests of the open porous $Ti_{62.5}Hf_{27.5}$ alloy and the $Ti_{62.5}Hf_{27.5}$_BPF composite. (Note: that numbers in the plots indicate corresponding strain rates in s^{-1}); and (d) Elastic modulus plotted against engineering strain for the interpenetrating-phase composites (Inset: loading-unloading stress-strain curve for $Ti_{62.5}Hf_{37.5}$_BPF).

The yield strength of the porous Ti_xHf_{100-x} samples varies from 100 MPa to 121 MPa. In its turn, the yield strength of the composites is several times higher as compared to the corresponding porous materials. This is clearly demonstrated in Fig. 3 a. Up to 266 MPa yield strength can be reached for the current set of interpenetrating-phase composites (Table 2). A comparison of yield strength values versus porous metal composition suggests

that the composites inherit strength from their metal scaffold. In particular, the porous $Ti_{50}Hf_{50}$ being stronger than the porous $Ti_{75}Hf_{25}$, forms the $Ti_{50}Hf_{50}$_BPF composite which is stronger than the $Ti_{75}Hf_{25}$_BPF composite.

Table 2. Mechanical properties of the porous Ti_xHf_{100-x} alloys and the interpenetrating-phase Ti_xHf_{100-x}_BPF composites.

Sample	**Young's modulus [GPa]**	**Yield strength [MPa]**
$Ti_{50}Hf_{50}$	8.5±1.3	121±12
$Ti_{62.5}Hf_{37.5}$	5.6±1.0	100±8
$Ti_{75}Hf_{25}$	6.4±0.5	120±6
$Ti_{50}Hf_{50}$_BPF	20.8±1.3	266±17
$Ti_{62.5}Hf_{37.5}$_BPF	15.6±0.7	229±14
$Ti_{75}Hf_{25}$_BPF	18.0±1.1	215±18
BPF	1.38±0.2	51±3

Along with the strength improvement, the polymer impregnation into the porous scaffolds leads to a several times higher stiffness of the composite materials compared to the porous ones (Table 2). For the current set of the as-prepared porous Ti_xHf_{100-x} alloys, Young's modulus values vary from about 6.4 GPa to 8.5 GPa. Interestingly, these Young's modulus values are more than an order of magnitude lower compared to those of their bulk counterparts [24,27] despite a relatively high solid fraction (54-59 vol.%) in the porous Ti_xHf_{100-x} alloys. The polymer impregnation into the porous $Ti_{62.5}Hf_{37.5}$ and $Ti_{75}Hf_{25}$ alloys leads to an increase of Young's modulus by a factor of 2.8. For example, the Young's modulus of $Ti_{50}Hf_{50}$_BPF is as high as 20.8 GPa. Moreover, Young's modulus as well as yield strength values of the current interpenetrating-phase composites exceed those of each constituent alone (Table 2). This confirms the observations reported for np-Au-polymer composites [28] as well as for Ti-polymer, TiZr-polymer, TiNb-polymer, and Zr-polymer composites [13,28]. The pronounced strengthening effect induced by polymer impregnation

may be explained by a change of deformation mode. Rather than densifying by a bending-dominated deformation, as in the porous metal, the ligaments in the composite deform along with an essentially volume-conserving macroscopic strain field [13]. Thus, infiltration of the polymer into nano-/microporous metallic scaffolds is an effective method for superior improvement of their mechanical performance.

The more delicate tuning of mechanical properties of the porous Ti_xHf_{100-x} alloys can be achieved by employing compressive prestraining. As it was mentioned above, the current porous Ti_xHf_{100-x} alloys exhibit a pronounced strain-hardening behavior (Fig. 3). Therefore, their yield strength and Young's modulus values can be optimized by compressive prestraining. Compressive stress-strain curves including load-unload cycles together with the Young's modulus plotted against plastic strain of the porous Ti_xHf_{100-x} alloys demonstrate this in Fig. 3 b. The yield strength and Young's modulus values increase at higher prestraining. Specifically, the yield strength of the porous $Ti_{75}Hf_{25}$ reaches about 400 MPa while the Young's modulus is about 33.7 GPa at the engineering strain of 0.25. In this work, the Young's modulus of the porous Ti_xHf_{100-x} can be tuned from about 5.6 GPa to 38.8 GPa by compressive prestraining (Fig. 3 b). These Young's modulus values are particularly remarkable, because they match those (0.1 GPa – 25 GPa) found for human bone [30,31].

The increasing values of Young's modulus of the porous Ti_xHf_{100-x} upon prestraining can be explained by the densification of the porous structure. The impregnation of polymers into the pore space prevents further microstructural densification and stabilizes the Young's modulus of the metal-polymer composites as it was reported in [13]. The dependence of Young's modulus on plastic predeformation of the current metal-polymer composites is demonstrated in Fig. 3 d. The Young's modulus of the composites remains almost unchanged at high values of strain. The conservation of Young's modulus at high strain rates indicates connectivity conservation of the metallic scaffolds in the composites instead of their disruption. Thus, the prestraining of the dealloying-based scaffolds with following polymer impregnation is promising for the fine optimization of mechanical properties, e.g. strength and stiffness, of the dealloying-based materials.

Besides the unique combination of moderate yield strength and low Young's modulus, the bone exhibits significant strain rate sensitivity becoming stronger and stiffer at higher strain rates [32,33]. The further characterization of the current materials is related to the evaluation of their strain rate sensitivity. To estimate the strain rate sensitivity, strain rate jump experiments were performed, see Fig. 3 c. The strain rate sensitivity is determined here as $m = \partial \ln\sigma / \partial \ln\dot{\varepsilon}$, where σ – strength and $\dot{\varepsilon}$ – strain rate. The *m* values of the porous materials are ranging from 0.014 to 0.015 for $Ti_{50}Hf_{50}$ and $Ti_{75}Hf_{25}$, respectively. In its turn, the *m* values of the composites are nearly three times higher than those of the porous counterparts ranging from 0.037 to 0.044. The increasing strain rate sensitivity of the composites is due to the viscoelastic properties of the infiltrated polymer. The *m* values of bone derived from the stress-strain curves reported by Crowninshiled and Pope [32] are in a range of 0.044 to 0.058 nearly matching those of the current composites. In other words, the yield strength of the interpenetrating-phase metal-polymer composites would notably increase at higher strain rates similarly to that of bone.

Fig. 4 shows the microstructure of the interpenetrating-phase composites after the compressive test. The polymer phase is clearly distinguishable in the current SEM micrographs. As can be seen, the polymer and metallic phases are deattached at some places. The number of such debondings (or microcracks) on the polished surface of the tested composites is relatively low. Similar debonding failure between gold and polymer phases was reported for the composite of nanoporous gold and polymer [34]. Based on experimental observations and modelling, it was suggested that the debonding occurs due to high strains in the polymer phase caused by the different mechanical properties of the gold and polymer phases and irregular geometries of ligaments [34]. Generally, the appearance of the debondings/microcracks in the current Ti_xHf_{100-x}_BPF composites indicates weak bonding between polymer and metallic phases. Moreover, these microcracks could be initiation sites of failure cracks in these composites. Therefore, it might be suggested that the further performance improvement of the interpenetrating-phase metal-polymer composites has to focus on strengthening the bonding between metal and polymer phases.

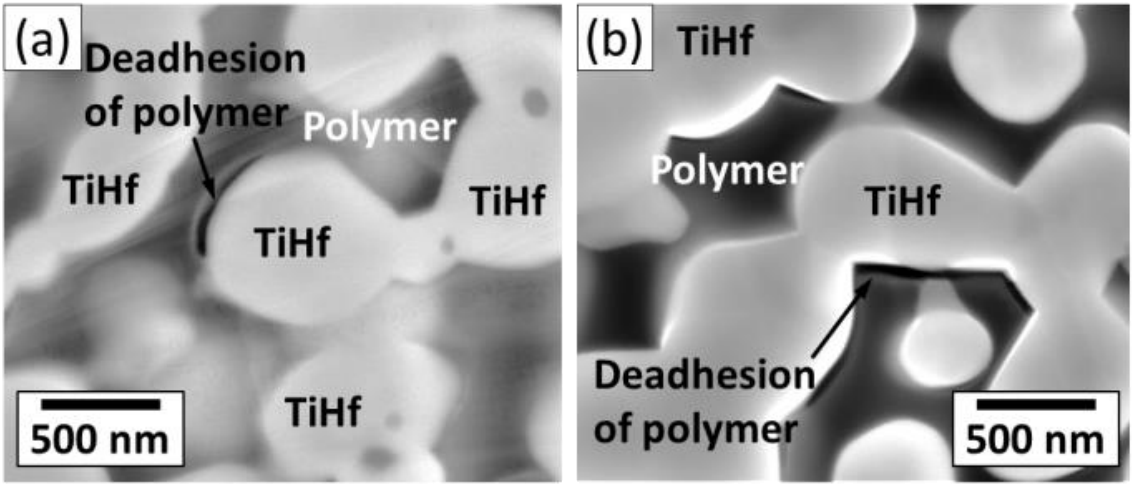

Fig. 4 Microstructure of the interpenetrating-phase Ti_xHf_{100-x}_BPF composites after deformation up to fracture. (a) $Ti_{50}Hf_{50}$_BPF; and (b) $Ti_{75}Hf_{25}$_BPF.

The current open porous Ti_xHf_{100-x} alloys and the Ti_xHf_{100-x}_BPF interpenetrating-phase composites represent a relatively new class of engineering materials. The strength and

stiffness parameters of the current dealloying-based materials occupy a previously unclaimed region at the Ashby diagram in the area of intermediate strength and low stiffness. This observation is in accordance with our earlier report in reference [13]. Moreover, the strain rate dependence of the interpenetrating-phase composite materials was estimated to be nearly similar to that of bone. The set of mechanical properties of the current dealloying-based materials, including intermediate yield strength, low Young's modulus, and high strain rate sensitivity, suggest opportunities for load-bearing implant applications. Additionally, the large hysteresis loop on the stress-strain curve during load-unloading tests (Figs. 3 b a and d) suggests some applications related to dissipation of mechanical energy upon cycling loading. As a benefit of the interconnected composite microstructure, the excessive heat forming during the energy absorption can be transferred through the metallic scaffold.

In summary, several open porous Ti_xHf_{100-x} alloys were synthesized by liquid metal dealloying using magnesium as the corrosive medium. The as-prepared porous Ti_xHf_{100-x} alloys exhibit good mechanical properties, including comparably high yield strength (from 100 to 121 MPa) and low Young's modulus (5.6 to 8.5 GPa). Moreover, the pronounced strain-hardening behavior and large deformability of these porous Ti_xHf_{100-x} alloys allow simultaneous tuning of their strength and stiffness properties by plastic prestraining. In particular, the Young's modulus of the porous Ti_xHf_{100-x} alloys was tuned in that way from about 5.6 GPa to 38.8 GPa. Additionally, to improve the mechanical performance of the porous Ti_xHf_{100-x} alloys, these were impregnated by the polymer (based on bisphenol F (BPF)) to form interpenetrating-phase metal-polymer composites. The yield strength values of the composites exceed those of bone reaching up to 266 MPa while their Young's modulus values (15.6 - 20.8 GPa) are matching those of bone. Moreover, the composites exhibit the high strain rate sensitivity inherited from the polymer phase with *m* values ranging from 0.037 to 0.044. This is similar to that of bone possessing *m* values in a range of 0.044 to 0.058. Thus, the developed interpenetrating-phase Ti_xHf_{100-x}_BPF composites demonstrate strong advantages to be considered for biomedical implant applications.

Acknowledgements

The funding by the Helmholtz Impuls- und Vernetzungsfonds via the Helmholtz - Chinese Academy of Sciences Joint Research Group “Nanoporous transition metals for strength and function – towards a cost-efficient materials base” under Grant number HCJRG-315 is gratefully acknowledged.

Literature

[1] M. Niinomi, Mechanical biocompatibilities of titanium alloys for biomedical applications., J. Mech. Behav. Biomed. Mater. 1 (2008) 30–42. doi:10.1016/j.jmbbm.2007.07.001.

[2] M. Niinomi, M. Nakai, J. Hieda, Development of new metallic alloys for biomedical applications., Acta Biomater. 8 (2012) 3888–903. doi:10.1016/j.actbio.2012.06.037.

[3] M. Geetha, A.K. Singh, R. Asokamani, A.K. Gogia, Ti based biomaterials, the ultimate choice for orthopaedic implants – A review, Prog. Mater. Sci. 54 (2009) 397–425. doi:10.1016/j.pmatsci.2008.06.004.

[4] I.V. Okulov, H. Wendrock, A.S. Volegov, H. Attar, U. Kühn, W. Skrotzki, et al., High strength beta titanium alloys: New design approach, Mater. Sci. Eng. A. 628 (2015) 297–302. doi:10.1016/j.msea.2015.01.073.

[5] I.V. Okulov, S. Pauly, U. Kühn, P. Gargarella, T. Marr, J. Freudenberger, et al., Effect of microstructure on the mechanical properties of as-cast Ti–Nb–Al–Cu–Ni alloys for biomedical application, Mater. Sci. Eng. C. 33 (2013) 4795–4801. doi:10.1016/j.msec.2013.07.042.

[6] I.V. Okulov, U. Kühn, T. Marr, J. Freudenberger, I.V. Soldatov, L. Schultz, et al., Microstructure and mechanical properties of new composite structured Ti–V–Al–Cu–Ni alloys for spring applications, Mater. Sci. Eng. A. 603 (2014) 76–83. doi:10.1016/j.msea.2014.02.070.

[7] I. V Okulov, A.S. Volegov, H. Attar, M. Bönisch, M. Calin, J. Eckert, Composition optimization of low modulus and high-strength TiNb-based alloys for biomedical applications, J. Mech. Behav. Biomed. Mater. 65 (2017) 866–871. doi:10.1016/j.jmbbm.2016.10.013.

[8] I.V. Okulov, M. Bönisch, A.S. Volegov, H. Shahabi Shakur, H. Wendrock, T. Gemming, et al., Micro-to-nano-scale deformation mechanism of a Ti-based dendritic-ultrafine eutectic alloy exhibiting large tensile ductility, Mater. Sci. Eng. A. (2016). doi:10.1016/j.msea.2016.11.082.

[9] I.V. Okulov, M. Bönisch, U. Kühn, W. Skrotzki, J. Eckert, Significant tensile ductility and toughness in an ultrafine-structured Ti68.8Nb13.6Co6Cu5.1Al6.5 bi-

modal alloy, Mater. Sci. Eng. A. 615 (2014) 457–463. doi:10.1016/j.msea.2014.07.108.

[10] I. V. Okulov, U. Kühn, T. Marr, J. Freudenberger, L. Schultz, C.-G. Oertel, et al., Deformation and fracture behavior of composite structured Ti-Nb-Al-Co(-Ni) alloys, Appl. Phys. Lett. 104 (2014) 071905. doi:10.1063/1.4865930.

[11] B.J.C. Luthringer, F. Ali, H. Akaichi, F. Feyerabend, T. Ebel, R. Willumeit, Production , characterisation , and cytocompatibility of porous titanium-based particulate scaffolds, (2013) 2337–2358. doi:10.1007/s10856-013-4989-z.

[12] K.G. Prashanth, K. Zhuravleva, I. Okulov, M. Calin, J. Eckert, A. Gebert, Mechanical and Corrosion Behavior of New Generation Ti-45Nb Porous Alloys Implant Devices, Technologies. 4 (2016) 33. doi:10.3390/technologies4040033.

[13] I. V Okulov, J. Weissmüller, J. Markmann, Dealloying-based interpenetrating-phase nanocomposites matching the elastic behavior of human bone, Sci. Rep. 7 (2017) 20. doi:10.1038/s41598-017-00048-4.

[14] T. Wada, K. Yubuta, A. Inoue, H. Kato, Dealloying by metallic melt, Mater. Lett. 65 (2011) 1076–1078. doi:10.1016/j.matlet.2011.01.054.

[15] T. Wada, A.D. Setyawan, K. Yubuta, H. Kato, Nano- to submicro-porous β-Ti alloy prepared from dealloying in a metallic melt, Scr. Mater. 65 (2011) 532–535. doi:10.1016/j.scriptamat.2011.06.019.

[16] J.W. Kim, M. Tsuda, T. Wada, K. Yubuta, S.G. Kim, H. Kato, Optimizing niobium dealloying with metallic melt to fabricate porous structure for electrolytic capacitors, Acta Mater. 84 (2015) 497–505. doi:10.1016/j.actamat.2014.11.002.

[17] I. McCue, B. Gaskey, P.A. Geslin, A. Karma, J. Erlebacher, Kinetics and morphological evolution of liquid metal dealloying, Acta Mater. 115 (2016) 10–23. doi:10.1016/j.actamat.2016.05.032.

[18] T. Wada, H. Kato, Three-dimensional open-cell macroporous iron, chromium and ferritic stainless steel, Scr. Mater. 68 (2013) 723–726. doi:10.1016/j.scriptamat.2013.01.011.

[19] P. Geslin, I. Mccue, J. Erlebacher, A. Karma, Topology-generating interfacial pattern formation during liquid metal dealloying, Nat. Commun. 6 (2015) 1–19.

doi:10.1038/ncomms9887.

[20] M. Heiden, D. Johnson, L. Stanciu, Surface modifications through dealloying of Fe-Mn and Fe-Mn-Zn alloys developed to create tailorable, nanoporous, bioresorbable surfaces, Acta Mater. 103 (2016) 115–127. doi:10.1016/j.actamat.2015.10.002.

[21] K. Sasaki, S. Osamu, N. Takahashi, Interface oral health science 2014: Innovative research on biosis-abiosis intelligent interface, Interface Oral Heal. Sci. 2014 Innov. Res. Biosis-Abiosis Intell. Interface. (2015) 1–351. doi:10.1007/978-4-431-55192-8.

[22] I. McCue, S. Ryan, K. Hemker, X. Xu, N. Li, M. Chen, et al., Size Effects in the Mechanical Properties of Bulk Bicontinuous Ta/Cu Nanocomposites Made by Liquid Metal Dealloying, Adv. Eng. Mater. 18 (2016) 46–50. doi:10.1002/adem.201500219.

[23] H. Matsuno, A. Yokoyama, F. Watari, M. Uo, T. Kawasaki, Biocompatibility and osteogenesis of refractory metal implants, titanium, hafnium, niobium, tantalum and rhenium, Biomaterials. 22 (2001) 1253–1262. doi:https://doi.org/10.1016/S0142-9612(00)00275-1.

[24] H. Sato, M. Kikuchi, M. Komatsu, O. Okuno, T. Okabe, Mechanical properties of cast Ti–Hf alloys, J. Biomed. Mater. Res. Part B Appl. Biomater. 72B (2005) 362–367. doi:10.1002/jbm.b.30169.

[25] H. Baker, ed., ASM Handbook: Alloy Phase Diagrams, ASM Internetional, 1992.

[26] K. Wang, A. Kobler, C. Kübel, H. Jelitto, G. Schneider, J. Weissmüller, Nanoporous-gold-based composites: toward tensile ductility, NPG Asia Mater. 7 (2015) e187. doi:10.1038/am.2015.58.

[27] Y.L. Zhou, M. Niinomi, T. Akahori, Dynamic Young's modulus and mechanical properties of Ti-Hf alloys, Mater. Trans. 45 (2004) 1549–1554. doi:10.2320/matertrans.45.1549.

[28] K. Wang, J. Weissmüller, Composites of nanoporous gold and polymer, Adv. Mater. 25 (2013) 1280–1284. doi:10.1002/adma.201203740.

[29] N. Mameka, K. Wang, J. Markmann, E.T. Lilleodden, J. Weissmüller, Nanoporous Gold—Testing Macro-scale Samples to Probe Small-scale Mechanical Behavior, Mater. Res. Lett. 3831 (2015) 1–10. doi:10.1080/21663831.2015.1094679.

[30] J.B. Park, J.D. Bronyino, Biomaterials: principles and applications, 2nd ed., CRC Press, Boca Raton, 2000.

[31] R.E. Smallman, R.J. Bishop, Chapter 13 - Biomaterials, in: R.E. Smallman, R.J. BiShop (Eds.), Mod. Phys. Metall. Mater. Eng. (Sixth Ed., Sixth edit, Butterworth-Heinemann, Oxford, 1999: pp. 394–405. doi:http://dx.doi.org/10.1016/B978-075064564-5/50013-6.

[32] R.D. Crowninshiled, M.H. Pope, The responce of compact bone in tension at various strain rates, Ann. Biomed. Eng. 2 (1974) 217–225.

[33] J.H. McElhaney, Dynamic response of bone and muscle tissue., J. Appl. Physiol. 21 (1966) 1231 LP – 1236. http://jap.physiology.org/content/21/4/1231.abstract.

[34] K. Hu, Micromechanical and Three-Dimensional Microstructural Characterization of Nanoporous Gold-Epoxy Composites, Technischen Universität Hamburg-Harburg, 2017.